

# Near-infrared aminocyanine dyes: synthesis, optical properties, and application to the preparation of fluorescent microspheres

Liang Yu · Tingting Li · Qiuling Wang · Lei Li · Ligong Chen

Received: 29 October 2012 / Accepted: 15 January 2013  
© Springer Science+Business Media Dordrecht 2013

**Abstract** Several near-infrared (NIR) fluorescent dyes based on aminocyanine have been designed, synthesized, and used for preparation of NIR fluorescent microspheres. Their spectral properties and pH-dependent optical characteristics were investigated. It was found that different substitution at the central position of the dyes led to diverse optical properties, with especially large effects on their spectroscopic properties. Spectroscopic responses of the fluorescent dyes to changes of pH were different. Under acidic conditions, the wavelengths of maximum absorption of the N-substituted cyanine dyes were clearly red shifted. Dyes with an N-substituted piperazine ring were the most sensitive. The fluorescent microspheres retained the properties of the parent dyes, making them suitable for applications in biological studies.

**Keywords** Near-infrared · pH-dependent · Fluorescent · Microsphere

## Introduction

Fluorescent labeling is one of the most common bioanalytical methods [1–4]. Highly uniform fluorescent microspheres are widely used in such methods, because of their unique properties resulting from their large surface-to-volume ratios and small sizes [5–7]. Some fluorescent dyes, for example, rhodamine and fluorescein, are often used to prepare fluorescent spheres [8], although such problems as limited

---

L. Yu · T. Li · L. Li · L. Chen (✉)  
School of Chemical Engineering and Technology, Tianjin University, Tianjin 300072,  
People's Republic of China  
e-mail: lgchen@tju.edu.cn

Q. Wang  
School of Pharmaceuticals and Biotechnology, Tianjin University, Tianjin 300072,  
People's Republic of China

visibility and background fluorescence, has hampered widespread application [9, 10]. As a result, use of near-infrared fluorescent labeling reagents and microspheres for biological applications has expanded rapidly in recent years. In optical imaging in the NIR region (700–900 nm) absorption by intrinsic photoactive biomolecules is low, which enables light to penetrate several centimeters into tissue, a depth which is sufficient for practical imaging for all small animal models [11–15]. Among organic near-infrared dyes, aminocyanines used as fluorescence labels and sensors of biomolecules *in vivo* have attracted much interest because their spectra reach the near-infrared (NIR) region [16–18]. Gabor Patonay et al. and Peng et al. developed cyanine dyes with large Stokes shifts (>140 nm), high photostability, and strong fluorescence which made them more suitable than conventional cyanine dyes as fluorescence probes [19–21].

Biochemical processes frequently involve protonation and deprotonation of biomolecules with concomitant changes in the pH of the medium [22–25]. As a result, there has been an increasing requirement for pH-sensitive fluorescent probes [26–29] and fluorescent microspheres [24, 25]. Only a few NIR fluorescent microspheres have been reported [25].

Herein, we describe a series of aminocyanine dyes prepared in the hope that introduction of different heterocyclic rings would lead to diverse optical properties. It was also envisaged that interaction of protons with the nitrogen atom on the central rings would result in different changes of the absorption and emission spectra. We also wished to devise a method for preparation of NIR fluorescent microspheres based on the cyanine dyes. All the aminocyanine dyes were characterized by NMR spectroscopy and mass spectrometry, and their optical properties were investigated by UV–visible and fluorescence spectroscopy. Their absorption and emission properties over eight pH units were also studied. The compounds had large Stokes shifts and strong fluorescence in the NIR region with high quantum yields. These properties are suitable for *in-vivo* imaging.

## Experimental

### Chemicals and instruments

All chemicals and reagents were commercially available and used without further purification. All solvents were carefully dried and freshly distilled by use of standard procedures.  $^1\text{H}$  NMR and  $^{13}\text{C}$  NMR spectra were recorded in  $\text{CDCl}_3$  on a Varian Inova 500-MHz NMR spectrometer using TMS as an internal standard. Mass spectra were obtained with Bruker Daltonics Autoflex tof/tofIII. UV–visible absorption spectra were recorded on a Perkin Elmer Lambda 750 spectrophotometer. Fluorescence spectra were obtained on a Varian Eclipse fluorescence spectrophotometer at room temperature. The environmental scanning electron images (ESEMs) were obtained by use of a XL30 environmental scanning electron microscope. Polystyrene microspheres with diameters of  $2.81 \pm 0.03 \mu\text{m}$  was obtained from Tianjin Baseline ChroTech Research Centre (China).

## Determination of quantum yield

The fluorescence quantum yields of the synthesized dyes were calculated relative to that of a standard solution of rhodamine B in ethanol ( $\varphi = 0.56$ ) and were determined by use of the equation [30]:

$$\varphi_x = \varphi_s (F_x / F_s) (A_s / A_x) (\lambda_{\text{exs}} / \lambda_{\text{exx}}) (n_x / n_s)^2$$

where  $\varphi$  is quantum yield,  $F$  is integrated area under the corrected emission spectrum,  $A$  is absorbance at the excitation wavelength,  $\lambda_{\text{ex}}$  is the excitation wavelength,  $n$  is the refractive index of the sample used for measurement and the subscripts  $x$  and  $s$  denote test and the standard, respectively.

## Synthesis

The structures of all the synthesized compounds are shown in Fig. 1.

2-Chloro-1-formyl-3-hydroxymethylene cyclohexene, *N*-methyl-2,3,3-trimethyl-indolenium, and IR786 (1) were prepared in accordance with a literature procedure [31] (Scheme 1).

## Compound 1

Yield 66%.  $^1\text{H}$  NMR (500 MHz,  $\text{CDCl}_3$ ):  $\delta$  1.71 (s, 12H), 1.93–1.98 (m, 2H), 2.73 (t, 4H,  $J = 5.97$  Hz), 3.74 (s, 6H), 6.20 (d, 2H,  $J = 14.10$  Hz), 7.18 (d, 2H,

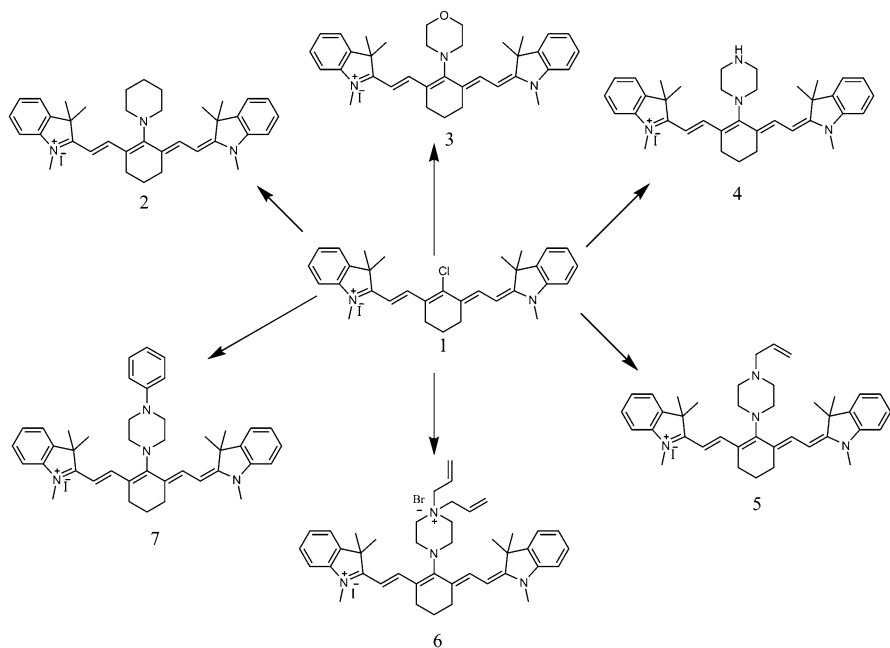
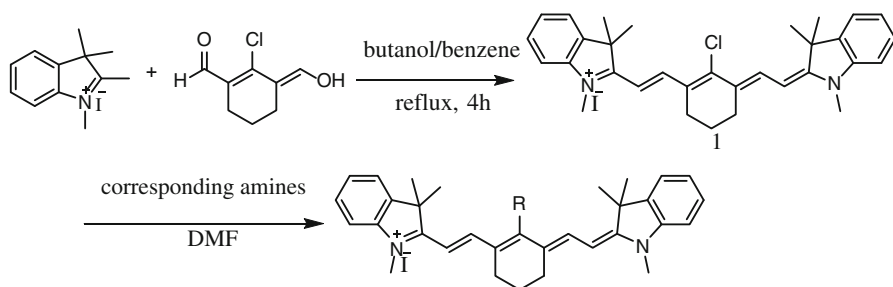


**Fig. 1** Functionalization of chlorocyanine dye 1



**Scheme 1** Synthetic route to aminocyanine dyes

$J = 7.33$  Hz), 7.24 (t, 2H,  $J = 7.12$  Hz), 7.36–7.41 (m, 4H), 8.34 (d, 2H,  $J = 14.10$  Hz).

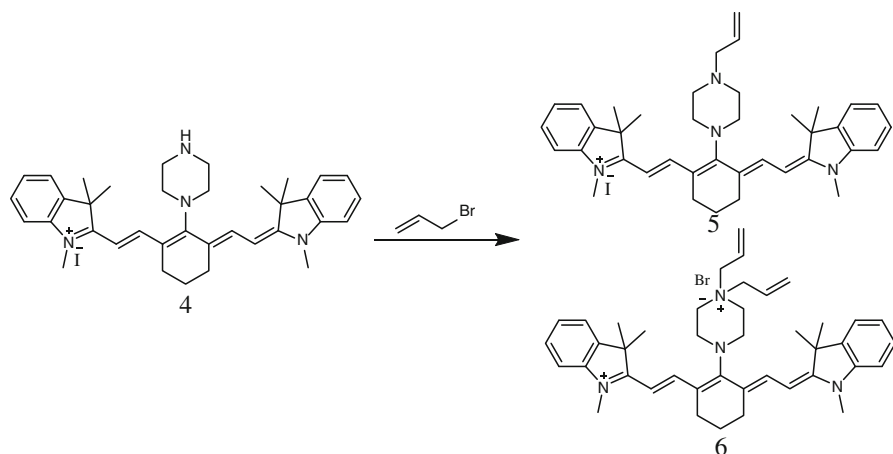
Synthesis of compounds **5** and **6** is shown in Scheme 2.

General procedure for synthesis of compounds **2**, **3**, **4**, and **7**

The corresponding heterocyclic compounds (2.0 mmol) were added to compound **1** (122 mg, 0.2 mmol) dissolved in anhydrous DMF (10 mL). The mixture was stirred at 80 °C for 2 h under a nitrogen atmosphere then concentrated. The residue was purified by silica gel chromatography with dichloromethane and methanol, then recrystallized from methanol and diethyl ether to afford a golden powder.

### Compound 2

Yield 83 %.  $^1\text{H NMR}$  (500 MHz,  $\text{CDCl}_3$ ):  $\delta$  1.66 (s, 12H), 1.84–1.91 (m, 2H), 2.50 (t, 4H,  $J = 5.97$  Hz), 3.15 (br, 6H), 3.49 (s, 6H), 3.85 (br, 4H), 5.72 (d, 2H,  $J = 13.14$  Hz), 6.98 (d, 2H,  $J = 7.33$  Hz), 7.11 (t, 2H,  $J = 7.12$  Hz), 7.31–7.34 (m, 4H),



**Scheme 2** Synthetic route to NIR dyes **5** and **6**

7.55 (d, 2H,  $J = 13.14$  Hz).  $^{13}\text{C}$  NMR (500 MHz,  $\text{CDCl}_3$ ):  $\delta$  21.89, 24.54, 25.13, 28.44, 29.16, 31.2, 47.90, 57.22, 95.48, 109.14, 122.26, 123.45, 124.14, 128.68, 140.01, 140.61, 143.74, 168.58, 175.93. HRMS: calculated for  $[\text{M} - \text{I}^-]$ : 532.3686, measured: 532.3685.

### Compound 3

Yield 33 %.  $^1\text{H}$  NMR (500 MHz,  $\text{CDCl}_3$ ):  $\delta$  1.67 (s, 12H), 1.81–1.86 (m, 2H), 2.52 (t, 4H,  $J = 6.43$  Hz), 3.57 (s, 6H), 3.72 (t, 4H,  $J = 4.28$  Hz), 3.97 (t, 4H,  $J = 4.28$  Hz), 5.86 (d, 2H,  $J = 13.49$  Hz), 7.04 (d, 2H,  $J = 7.93$  Hz), 7.14 (t, 2H,  $J = 7.44$  Hz), 7.29–7.34 (m, 4H), 7.71 (d, 2H,  $J = 13.49$  Hz).  $^{13}\text{C}$  NMR (500 MHz,  $\text{CDCl}_3$ ): 21.90, 25.42, 29.09, 31.81, 48.33, 55.37, 68.57, 97.46, 109.88, 122.10, 124.14, 125.43, 128.81, 140.02, 140.73, 143.46, 170.11, 172.34. HRMS: calculated for  $[\text{M} - \text{I}^-]$ : 534.3479, measured: 534.3485.

### Compound 4

Yield 65 %.  $^1\text{H}$  NMR (500 MHz,  $\text{CDCl}_3$ ):  $\delta$  1.69 (s, 12H), 1.82–1.85 (m, 2H), 2.49 (t, 4H,  $J = 6.29$  Hz), 3.33 (br, 4H), 3.54 (s, 6H), 4.04 (br, 4H), 5.73 (d, 2H,  $J = 13.26$  Hz), 7.00 (d, 2H,  $J = 7.83$  Hz), 7.12 (t, 2H,  $J = 7.42$  Hz), 7.31–7.34 (m, 4H), 7.66 (d, 2H,  $J = 13.26$  Hz).  $^{13}\text{C}$  NMR (500 MHz,  $\text{CDCl}_3$ ):  $\delta$  21.87, 25.12, 25.98, 28.72, 31.45, 46.04, 48.21, 53.07, 62.49, 97.54, 110.48, 122.63, 123.93, 124.74, 128.78, 140.71, 140.83, 143.74, 169.97, 171.32. HRMS: calculated for  $[\text{M} - \text{I}^-]$ : 533.3639, measured: 533.3635.

### Compound 7

Yield 68 %.  $^1\text{H}$  NMR (500 MHz,  $\text{CDCl}_3$ ):  $\delta$  1.65 (s, 12H), 1.84–1.89 (m, 2H), 2.55 (t, 4H,  $J = 6.47$  Hz), 3.47 (br, 4H), 3.57 (s, 6H), 3.88 (t, 4H,  $J = 4.41$  Hz), 5.87 (d, 2H,  $J = 13.46$  Hz), 6.99 (t, 1H,  $J = 7.32$  Hz), 7.04 (t, 4H,  $J = 7.60$  Hz), 7.13 (t, 2H,  $J = 7.46$  Hz), 7.26–7.28 (m, 2H), 7.31–7.38 (m, 4H), 7.74 (d, 2H,  $J = 13.46$  Hz).  $^{13}\text{C}$  NMR (500 MHz,  $\text{CDCl}_3$ ):  $\delta$  21.90, 25.42, 29.13, 31.83, 48.37, 50.88, 51.91, 54.81, 54.93, 97.34, 109.87, 117.37, 122.14, 124.01, 125.53, 128.89, 129.87, 140.25, 141.84, 143.46, 170.12, 172.74. HRMS: calculated for  $[\text{M} - \text{I}^-]$ : 609.3952, measured: 609.3949.

### Synthesis of compound 5

Allyl bromide (238 mg, 2.0 mmol) and triethylamine (40 mg, 0.4 mmol) were added to compound 4 (132 mg, 0.2 mmol) dissolved in DMF (10 mL). The mixture was stirred at 65 °C for 1 h under a nitrogen atmosphere. The solvent was removed under reduced pressure, then the crude product was purified by silica gel chromatography with dichloromethane and methanol (20/1) ( $v/v$ ), and 5 was obtained as a golden powder (80 mg, 57 %).  $^1\text{H}$  NMR (500 MHz,  $\text{CDCl}_3$ ):  $\delta$  1.66 (s, 12H), 1.81–1.86 (m, 2H), 2.50 (t, 4H,  $J = 6.05$  Hz), 2.97 (br, 4H), 3.42–3.47 (m, 2H), 3.56 (s, 6H), 3.90 (br, 4H), 5.34–5.43 (m, 2H), 5.80 (d, 2H,  $J = 13.18$  Hz), 6.02 (br, 1H), 7.03 (d, 2H,  $J = 7.81$  Hz), 7.13 (t, 2H,  $J = 7.23$  Hz), 7.31–7.35 (m, 4H), 7.64 (d, 2H,  $J = 13.18$  Hz).  $^{13}\text{C}$  NMR (500 MHz,  $\text{CDCl}_3$ ):  $\delta$  21.81, 25.14, 28.94, 31.55, 31.76, 48.17, 53.47, 54.18, 54.62, 61.30, 96.46, 109.43, 122.01,

123.6, 124.6, 128.53, 140.01, 141.47, 143.32, 170.04, 173.2, HRMS: calculated for  $[M - I^-]$ : 573.3952, measured: 573.3955.

### Synthesis of compound 6

Allyl bromide (238 mg, 2 mmol) and triethylamine (40 mg, 0.4 mmol) were added to compound **4** (132 mg, 0.2 mmol) dissolved in DMF (10 mL). The mixture was stirred at 65 °C for 3 h under a nitrogen atmosphere and concentrated. The residue was then purified by silica gel chromatography with dichloromethane and methanol, to afford a golden needle powder **6** (74 mg, 45 %).  $^1\text{H}$  NMR (500 MHz,  $\text{CDCl}_3$ ):  $\delta$  1.68 (s, 12H), 1.99–2.02 (m, 2H), 2.59 (t, 4H,  $J = 6.05$  Hz), 3.47 (s, 6H), 4.20 (br, 4H), 4.58 (d, 4H,  $J = 5.76$  Hz), 4.72 (br, 4H), 5.52 (d, 2H,  $J = 13.09$ ), 5.85–5.87 (m, 2H), 6.07–6.13 (m, 4H), 6.91 (d, 2H,  $J = 7.89$  Hz), 7.08 (t, 2H,  $J = 7.44$  Hz), 7.26–7.30 (m, 4H), 7.52 (d, 2H,  $J = 13.09$  Hz).  $^{13}\text{C}$  NMR (500 MHz,  $\text{CDCl}_3$ ):  $\delta$  21.24, 27.12, 29.18, 31.65, 46.10, 48.12, 56.84, 58.31, 61.47, 952.4, 108.74, 122.15, 123.18, 123.26, 128.15, 131.20, 138.44, 139.96, 143.56, 168.60, 174.69. HRMS: calculated for  $[M - I^-]/2$ : 307.2169, measured: 307.2183.

### Preparation of fluorescent microspheres

PS beads were dispersed in ethanol by sonication to give a completely monodisperse microsphere system. After ultracentrifugation, the PS beads (8 mg/mL) were suspended in phosphate-buffered saline (PBS) and a solution of the dye in ethanol was added. The mixture was then subjected to ultrasonic irradiation for 8 h. The microspheres were then rinsed with PBS then centrifuged (5,000 rev/min) to remove unabsorbed dye.

## Results and discussion

### Synthesis of fluorescent dyes

Because the purpose of this work was to investigate the effect of different nitrogen-containing rings on the cyanine NIR dyes, first, we synthesized cyanine containing only a simple heterocyclic ring at the middle of the chain. On the basis of the above work, heterocyclic rings with different groups were also introduced into the dyes. All the designed fluorescent dyes were successfully obtained in accordance with the synthetic pathways described in Schemes 1 and 2. The structures of the synthesized compounds were confirmed by  $^1\text{H}$  and  $^{13}\text{C}$  NMR and mass spectrometry.

### Spectral properties of the synthesized cyanine dyes

The UV–visible and fluorescence spectra of the dyes are depicted in Figs. 2 and 3. It is obvious there are three general features of the spectra of dyes **2**, **3**, **4**, and **7**. First, they all have broad and fairly structureless fluorescence spectra. Second, large Stokes shifts ( $>90$  nm) are observed. Third, there is no mirror image relationship between the absorption and fluorescence spectra. These features are in agreement

with previous reports on aminocyanine dyes and result from intramolecular charge transfer (ICT) [32–34]. Dyes **5** and **6** have two of these features only, the exception being the Stokes shifts, which are only 34 and 44 nm, respectively.

The maximum absorption wavelengths ( $\lambda_{\max}$ ) of these dyes are in the range 666–769 nm (Table 1). When the central chlorine is replaced by piperazine, morpholine, and mono-substituted piperazine, obvious bathochromic shifts occur in the wavelengths of maximum absorption ( $\lambda_{\max}$ ) (from 22 to 103 nm) and the wavelengths of maximum emission ( $\lambda_{\text{em}}$ ) (from approx. 3 to 32 nm) compared with dye **2**. The molar extinction coefficient and fluorescence quantum yield of dyes **3**, **4**, **5**, and **7** are similar to those of dye **2**, whereas that of dye **6** is larger. Dyes **5** and **6**, which are synthesized from dye **4**, have unique spectral properties. When the first allyl group is introduced into dye **4**, an interesting change is observed in the absorption spectrum—the absorption peak at the longer wavelength becomes stronger than those for dyes **3** and **7**, and is the main absorption peak. After introduction of the second allyl group, an obvious increase is found in the absorbance intensity of dye **6**, and the extinction coefficient become  $2.03 \times 10^5$  ( $\text{M}^{-1} \text{cm}^{-1}$ ), compared with  $0.75 \times 10^5$  ( $\text{M}^{-1} \text{cm}^{-1}$ ) for dye **2**. Also, a difference appears in the emission spectra; the wavelength of maximum emission increases to 813 nm. These results indicate that substitution of the central chlorine with different nitrogen heterocyclic rings strongly affects the wavelength of maximum absorption and the absorbance intensity, and contributes substantially to the emission spectra. Details of the optical properties of the dyes are summarized in Table 1.

#### pH-dependent optical properties

To reveal the importance of medium pH to the optical properties of these dyes, their spectra were recorded in 50:50 (v/v) water–ethanol from pH 2.0 to 12.0, adjusted by addition of 1 M HCl or NaOH. The results are summarized in Figs. 4, 5, 6, and 7.

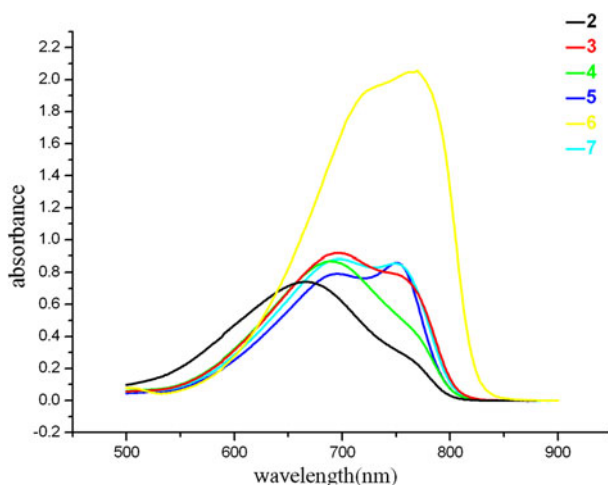


**Fig. 2** Absorption spectra of the dyes ( $10^{-5}$  mol  $\text{L}^{-1}$  in methanol)

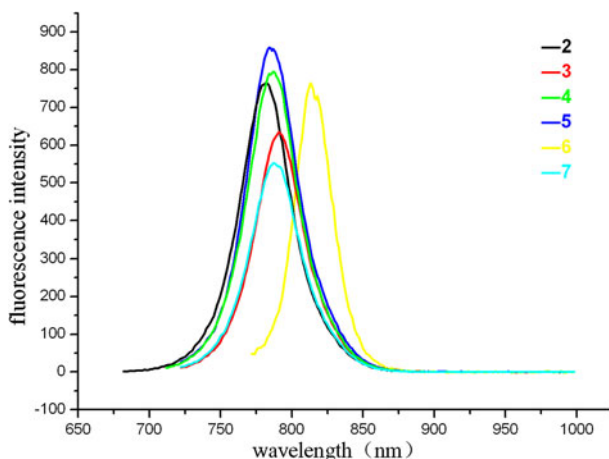


**Fig. 3** Emission spectra of the dyes ( $10^{-5}$  mol L $^{-1}$  in methanol)

It is obvious that these dyes can be divided into two types on the basis of trends in pH-dependent changes of their spectral properties. The first group is dyes **2**, **3**, and **7**; their absorption intensity becomes weaker with decreasing pH and their wavelengths of maximum emission and fluorescence intensity hardly change on protonation or deprotonation (Fig. 4). The difference between them is the sensitivity. For the other group, dyes **4**, **5**, and **6**, the trend is completely different. The absorption intensity becomes stronger with decreasing pH. At pH 6.24, dye **4** has a broad absorption band at 710 nm and a smaller band at 765 nm (Fig. 5). At higher pH, the wavelength of maximum absorption blue shifts to 687 nm. Above pH 7.39, no further changes in the absorption band can be observed, except for a slight decrease of absorption intensity with increasing pH. Under acid conditions, the absorption red shifts to 769 nm and intensity increases substantially. The trend with changing pH is the same for compound **5**, but it is not as sensitive as dye **4**. Only below pH 4.72 does the absorption band at 710 nm appear (Fig. 6). For dye **5** intensity changes only are observed. With regard to fluorescence properties, intensity for dyes **4**, **5**, and **6** become stronger with increasing pH. Dye **5** fluoresces weakly at 805 nm (Fig. 6) below pH 4.72. At pH 6.02, the fluorescence becomes

**Table 1** UV–visible fluorescent data of the dyes

Dye	$\lambda_{\max}$ (nm)	Extinction coefficient ( $M^{-1} \text{ cm}^{-1}$ )	$\lambda_{\text{ex}}$ (nm)	$\lambda_{\text{em}}$ (nm)	Stokes shifts (nm)	$\phi$
<b>2</b>	666	$0.75 \times 10^5$	666	781	115	0.18
<b>3</b>	693	$0.94 \times 10^5$	693	791	98	0.13
<b>4</b>	688	$0.87 \times 10^5$	688	787	99	0.16
<b>5</b>	750	$0.94 \times 10^5$	695	784	34	0.11
<b>6</b>	769	$2.03 \times 10^5$	700	813	44	0.08
<b>7</b>	697	$0.95 \times 10^5$	697	787	90	0.14

Conc.  $10^{-5}$  mol L $^{-1}$  in methanol

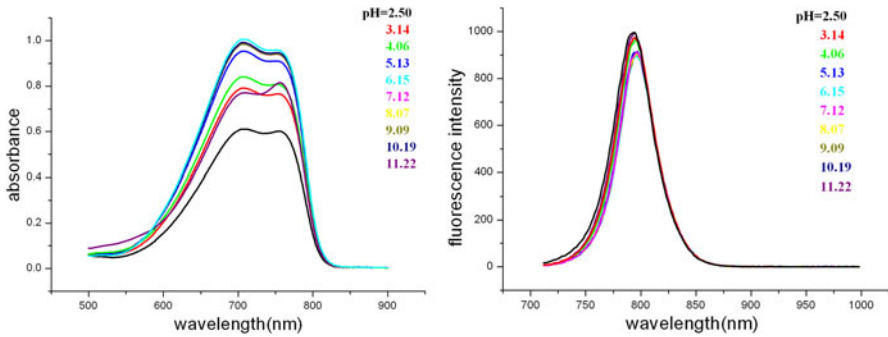


**Fig. 4** Absorption (*left*) and emission (*right*) spectra of **3** at different pH

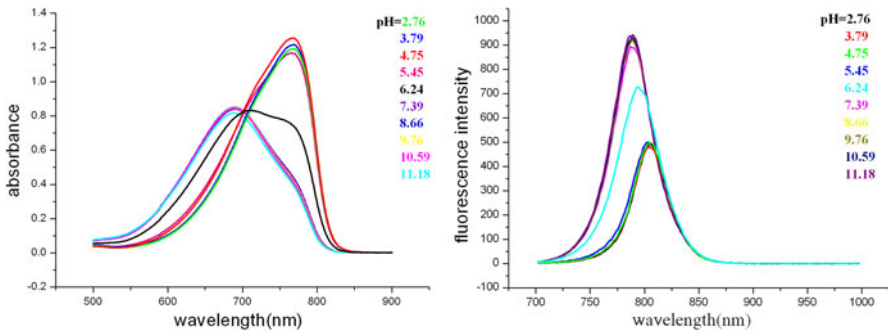


**Fig. 5** Absorption (*left*) and emission (*right*) spectra of **4** at different pH

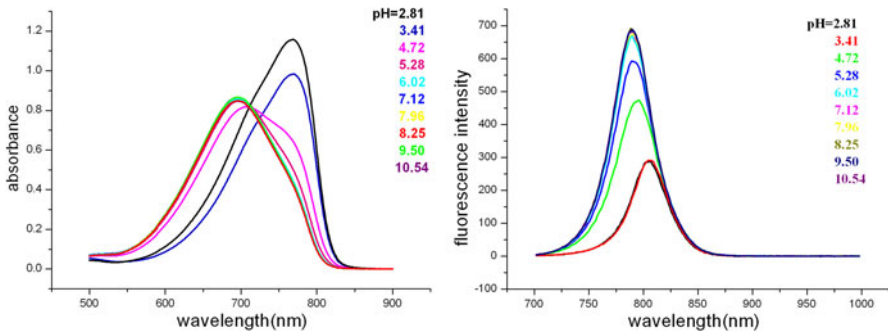


**Fig. 6** Absorption (*left*) and emission (*right*) spectra of **5** at different pH

much stronger and blue-shifts to 790 nm. Further increasing pH does not increase the emission intensity. The trend is the same for dyes **4** and **6**.

It has been reported that amidation of aminocyanine dyes can induce a substantial red-shift in absorption [28], which suggests that when protonation occurs at the two nitrogen atoms of such aminocyanines, a red shift of the absorption peak will occur owing to a

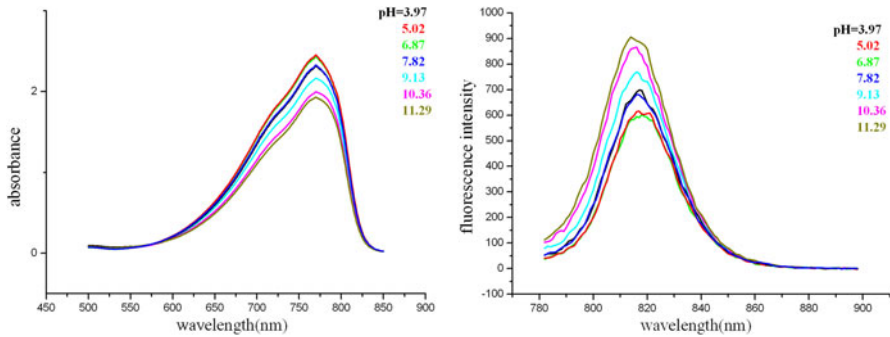


**Fig. 7** Absorption (*left*) and emission (*right*) spectra of **6** at different pH

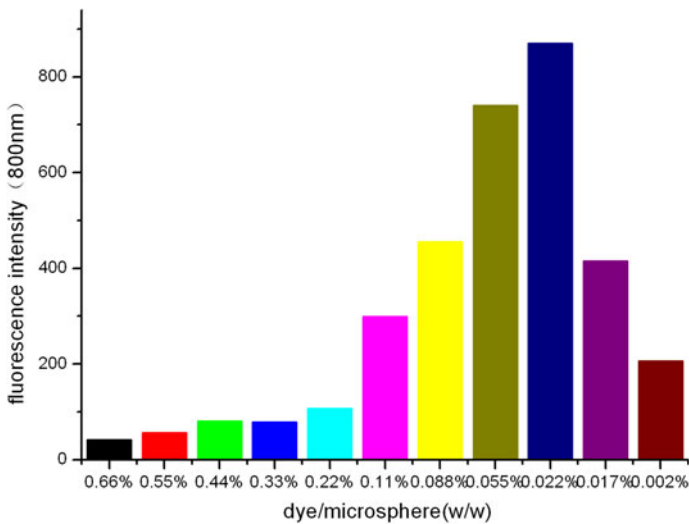


**Fig. 8** Dependence of fluorescence intensity of microspheres on dye-to-microsphere ratio (dye **7**)

decrease of the electron-donating ability of the amine. This behavior is observed for dyes **4** and **5**. Dye **6** is a modification of **5**. After introduction of the second allyl group, protonation is unable to occur at the two nitrogen atoms. The presence of phenyl in compound **7** may be the reason it differs from this trend. Phenyl makes the nitrogen atom of the piperazine less basic by conjugation, and it is more rigid than the allyl group.

#### Preparation and spectral properties of fluorescent microspheres

After investigation of their optical properties the dyes were used for preparation of fluorescent microspheres. Dye **7** was chosen as the first to be loaded on to the PS bead, because there is a phenyl group on the piperazidine ring which gave it greater affinity for the PS bead. The absorption method was chosen instead of copolymerization, because of the instability of cyanine dyes during the copolymerization process. This method has advantages over others because bead size and shape and

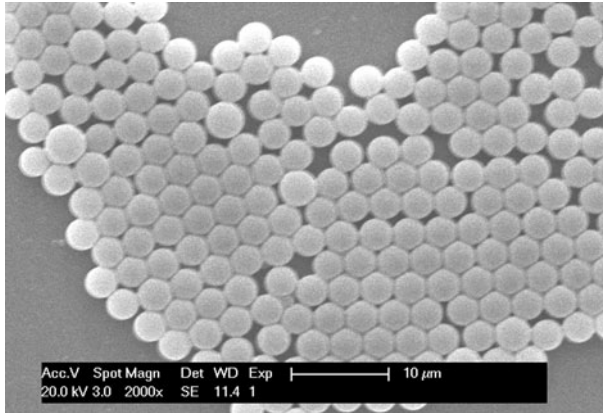


**Fig. 9** ESEM image of fluorescent microsphere based on dye 7

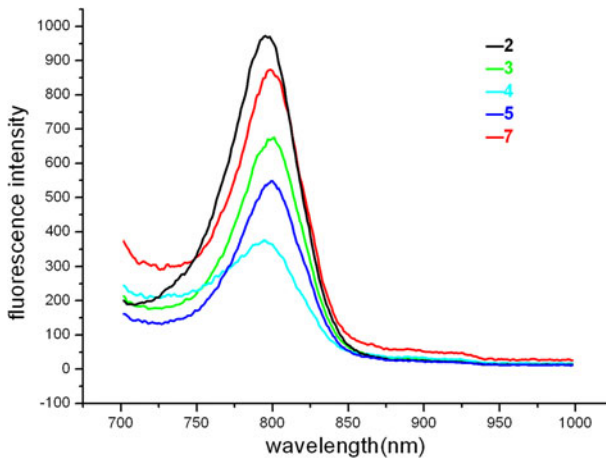


**Fig. 10** Emission spectra of different microspheres

**Table 2** Optical characteristics of the dyes and fluorescent microspheres

Dye	$\lambda_{em1}$ (nm) (dye)	$\lambda_{em2}$ (nm) (PS bead)	$\lambda_{em2} - \lambda_{em1}$ (nm)
2	781	796	15
3	791	800	9
4	787	795	8
5	784	800	16
7	787	797	10

fluorescence quenching can be controlled [35]. To achieve the highest fluorescence intensity, fluorescent microspheres with different ratios of dye 7 and PS bead were prepared. As can be seen from Fig. 8, the fluorescence intensity reached a

maximum when the ratio was 0.022 %. When the ratio decreased from 0.66 to 0.022 %, the fluorescence intensity at 800 nm increased from 42 to 870, and the intensity decreased with the continuous decrease of the ratio. The ESEM image (Fig. 9) showed that the microspheres were highly monodispersed. We therefore chose the ratio 0.022 %. The other fluorescent microspheres were prepared by use of the same method. The emission spectra are depicted in Fig. 10.

All the microspheres were obtained successfully and their spectral properties were studied. Investigations were performed in PBS, an aqueous medium often used in biological studies. As can be seen from Fig. 10, the microspheres had fluorescence profiles very similar to those of the parent dyes in methanol (Fig. 3), except for slight red shifts, which are listed in Table 2. The emission wavelengths were all approximately 800 nm, which were in the NIR range. Fortunately, the fluorescent microspheres retained the property of pH-sensitivity in aqueous media [36]. The emission intensity increased sharply as medium pH increased. Fluorescence intensity varied with the changes of pH, making it suitable for applications in biological studies.

## Conclusion

On the basis of this investigation of the absorption and fluorescence properties of these cyanine dyes, and their optical response to different pH, we can conclude that substitution of the chloro group with simple heterocyclic structures can lead to diverse optical properties. When piperidine is substituted by piperazine and morpholine, a red-shift is observed in the wavelength of maximum absorption ( $\lambda_{\max}$ ), with increased absorption and a decrease in fluorescence quantum yield. Modification of the heterocycles at the middle position also has a large effect on the optical properties of cyanine dyes. Furthermore, substituted piperazine incorporated into the fluorophore resulted in a wealth of pH-dependent optical properties, the absorption and fluorescence characteristic of the new dyes depending substantially on their molecular structures.

A method for preparation of NIR cyanine fluorescent microspheres is reported. Some of the synthesized dyes were used for preparation of fluorescent microspheres. The microspheres obtained had good optical properties. Most important, the aminocyanine-loaded microspheres were highly sensitive to changes in the pH of aqueous solutions, making them suitable for applications in biological studies.

## References

1. M.R. Mazières, F. Wetz, J. Bellan, J.G. Wolf, *Dyes Pigments* **56**, 231–238 (2003)
2. M.R. Mazières, C. Duprat, J. Bellan, J.G. Wolf, *Dyes Pigments* **74**, 404–409 (2007)
3. M. Sameiro, T. Gonçalves, *Chem. Rev.* **109**, 190–212 (2009)
4. P. Wellington, M. Zdravka, M. Anna, *Bioconj. Chem.* **16**, 735–740 (2005)
5. G.M. Qiu, Y.Y. Xu, B.K. Zhu, G.L. Qiu, *Biomacromolecules* **6**, 1041–1047 (2005)
6. A. Salinas-Castillo, M. Campubí-Robles, R. Mallavia, *Chem. Commun.* **46**, 1263–1265 (2010)

7. X.Q. Dong, Y.H. Zheng, Y.B. Huang, X.S. Chen, X.B. Jing, *Anal. Biochem.* **405**, 207–212 (2010)
8. Q.H. Liu, J. Liu, J.C. Guo, X.L. Yan, D.H. Wang, L.G. Chen, *J. Mater. Chem.* **19**, 2018–2025 (2009)
9. J.H. Wosnick, J.H. Liao, T.M. Swager, *Macromolecules* **38**, 9287–9290 (2005)
10. N. Insin, J.B. Tracy, H. Lee, J.P. Zimmer, R.M. Westervelt, M.G. Bawendi, *ACS Nano* **2**, 197–202 (2008)
11. A. Mishra, R.K. Behera, P.K. Behera, B.K. Mishra, G.B. Behera, *Chem. Rev.* **100**, 1973–2011 (2000)
12. R. Weissleder, V. Ntziachristos, *Nat. Med.* **9**, 123–128 (2003)
13. R. Raghavachari, *Near-Infrared Applications in Biotechnology* (Marcel Dekker, New York, 2001)
14. A. Zaheer, R.E. Lenkinski, A. Mahmood, A.G. Jones, L.C. Cantley, J.V. Frangioni, *Nat. Biotechnol.* **19**, 1148–1154 (2001)
15. A. Matsui, K. Umezawa, Y. Shindo, T. Fujii, K. Suzuki, *Chem. Commun.* **47**, 10407–10409 (2011)
16. C.Q. Zhu, Y.Q. Wu, H. Zheng, *Anal. Sci.* **20**, 945–949 (2004)
17. T. Slavnova, H. Görner, A.K. Chibisov, *J. Phys. Chem. B* **111**, 10023–10031 (2007)
18. G.Y. Guralchuk, A.V. Sorokin, I.K. Katrunov, S.L. Yefimova, *J. Fluoresc.* **17**, 370–376 (2007)
19. S. Lucjan, L. Malgorzata, P. Gabor, *J. Org. Chem.* **57**, 4578–4580 (1992)
20. Z.R. Zhang, S. Achilefu, *Org. Lett.* **6**, 2067–2070 (2004)
21. X.J. Peng, F.L. Song, E.H. Lu, Y.N. Wang, *J. Am. Chem. Soc.* **127**, 4170–4171 (2005)
22. M.R. Mazières, C. Duprat, J.G. Wolf, A.D. Roshal, *Dyes Pigments* **80**, 355–360 (2009)
23. S.D. Perez, E.D. Collado, F. Mollinedo, *J. Biol. Chem.* **270**, 6235–6242 (1995)
24. R.A. Gottlieb, A. Dosanjh, *Proc. Natl. Acad. Sci. USA* **93**, 3587–3591 (1996)
25. J.Y. Han, K. Burgess, *Chem. Rev.* **110**, 2709–2728 (2010)
26. B. Tang, F. Yu, P. Li, L. Tong, X. Duan, T. Xie, X. Wang, *J. Am. Chem. Soc.* **131**, 3016–3023 (2009)
27. E.J. Adie, S. Kalinka, L. Smith, M.J. Francis, A. Marengi, *Bio Techniques* **33**, 1152–1157 (2002)
28. T. Myochin, K. Kiyose, K. Hanaoka, T. Nagano, *J. Am. Chem. Soc.* **133**, 3401–3409 (2011)
29. K. Kiyose, S. Aizawa, E. Sasaki, H. Kojima, T. Nagano, *Chem. Eur. J.* **15**, 9191–9200 (2009)
30. L. Wang, J.L. Fan, X.Q. Qiao, X.J. Peng, B. Dai, *J. Photochem. Photobiol. A* **210**, 168–172 (2010)
31. L. David, J. Gallaher, J. Mitchell, *Analyst* **124**, 1541–1546 (1999)
32. A.B. Descalzo, K. Rurack, *Chem. Eur. J.* **15**, 3173–3185 (2009)
33. C.A. Benniston, A. Harriman, J.D. Lawrie, A. Mayeux, *Phys. Chem. Chem. Phys.* **6**, 51–57 (2004)
34. K. Kaneda, T. Arai, *Photochem. Photobiol. Sci.* **4**, 402–406 (2003)
35. D. Nagao, N. Anzai, Y. Kobayashi, S.C. Gu, M. Konno, *J. Colloid, Interface Sci.* **298**, 232–237 (2006)
36. L. Yu, Q.L. Wang, T.T. Li, L.G. Chen, *J. Chem. Res.* **36**, 632–634 (2012)